

## Accepted Manuscript

Design and synthesis of piperazine acetate podophyllotoxin ester derivatives targeting tubulin depolymerization as new anticancer agents

Wen-Xue Sun, Ya-Jing Ji, Yun Wan, Hong-Wei Han, Hong-Yan Lin, Gui-Hua Lu, Jin-Liang Qi, Xiao-Ming Wang, Yong-Hua Yang

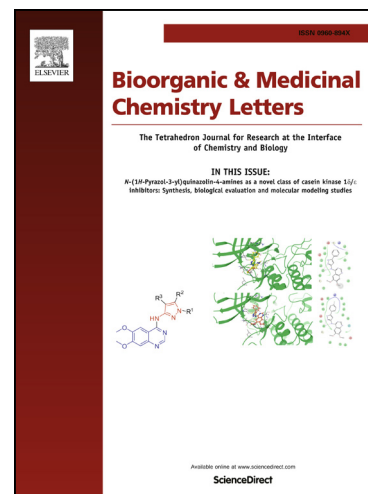
PII: S0960-894X(17)30754-0  
DOI: <http://dx.doi.org/10.1016/j.bmcl.2017.07.047>  
Reference: BMCL 25160

To appear in: *Bioorganic & Medicinal Chemistry Letters*

Received Date: 22 May 2017  
Revised Date: 3 July 2017  
Accepted Date: 18 July 2017

Please cite this article as: Sun, W-X., Ji, Y-J., Wan, Y., Han, H-W., Lin, H-Y., Lu, G-H., Qi, J-L., Wang, X-M., Yang, Y-H., Design and synthesis of piperazine acetate podophyllotoxin ester derivatives targeting tubulin depolymerization as new anticancer agents, *Bioorganic & Medicinal Chemistry Letters* (2017), doi: <http://dx.doi.org/10.1016/j.bmcl.2017.07.047>

This is a PDF file of an unedited manuscript that has been accepted for publication. As a service to our customers we are providing this early version of the manuscript. The manuscript will undergo copyediting, typesetting, and review of the resulting proof before it is published in its final form. Please note that during the production process errors may be discovered which could affect the content, and all legal disclaimers that apply to the journal pertain.





## Design and synthesis of piperazine acetate podophyllotoxin ester derivatives targeting tubulin depolymerization as new anticancer agents

Wen-Xue Sun,<sup>a,b</sup> Ya-Jing Ji,<sup>a,b</sup> Yun Wan,<sup>a,b</sup> Hong-Wei Han,<sup>a,b</sup> Hong-Yan Lin,<sup>a,b</sup> Gui-Hua Lu<sup>a,b</sup> Jin-Liang Qi,<sup>a,b,\*</sup> Xiao-Ming Wang<sup>a,b,\*</sup> and Yong-Hua Yang<sup>a,b,\*</sup>

<sup>a</sup>State Key Laboratory of Pharmaceutical Biotechnology, NJU-NJFU Joint Institute of Plant Molecular Biology, Nanjing University, Nanjing, 210023, China

<sup>b</sup>Co-Innovation Center for Sustainable Forestry in Southern China, Nanjing Forestry University, Nanjing, 210037, China

E-mails of corresponding authors: YHY: yangyh@nju.edu.cn, XMW: wangxm07@nju.edu.cn, JLQ: qijl@nju.edu.cn

### ABSTRACT

In this paper, a series of podophyllotoxin piperazine acetate ester derivatives were synthesized and investigated due to their antiproliferation activity on different human cancer cell lines. Among the congeners, **C5** manifested prominent cytotoxicity towards the cancer cells, without causing damage on the non-cancer cells through inhibiting tubulin assembly and having high selectivity causing damage on the human breast (MCF-7) cell line ( $IC_{50} = 2.78 \pm 0.15 \mu M$ ). Treatments of MCF-7 cells with **C5** resulted in cell cycle arrest in G2/M phase and microtubule network disruption. Moreover, regarding the expression of cell cycle relative proteins CDK1, a protein required for mitotic initiation was up-regulated. Besides, Cyclin A, Cyclin B1 and Cyclin D1 proteins were down-regulated. Meanwhile, it seems that the effect of **C5** on MCF-7 cells apoptosis inducing was observed to be not obvious enough. In addition, docking analysis demonstrated that the congeners occupy the colchicine binding pocket of tubulin.

2017 Elsevier Ltd. All rights reserved.

#### Keywords:

Podophyllotoxin piperazine acetate ester derivatives;  
Cytotoxicity  
Cell cycle  
Microtubule network  
Modeling

Microtubules (MTs), composed of  $\alpha/\beta$ -tubulin, are found around the cytoplasm, which are also crucial component of the cytoskeleton. The  $\alpha$ -tubulin and  $\beta$ -tubulin are the important members of the tubulin family and the most highly conserved eukaryotic proteins<sup>1</sup>. MTs are multifunctional in their function such as maintaining structure of the cell, chromosomal segregation, protein trafficking and mitosis<sup>2</sup>. In most cases, MTs are continuously experiencing the process of polymerization and de-polymerization, and thus in dynamic equilibrium with tubulin dimer<sup>3</sup>. Disruption of the dynamic equilibrium blocks the cell division machinery at mitosis and subsequently programmed cell death. Therefore, microtubules have been considered as being a promising target of antitumor drugs<sup>1</sup>. At present, it is admitted that microtubule possess three binding sites, respectively, the taxane domain, the colchicine domain and the vinca domain<sup>4</sup>. Colchicine was the first drug known to bind to tubulin, and indeed tubulin was originally isolated through its ability to bind colchicine<sup>4</sup>. Literature searching

shows that hundreds of potential colchicine binding site inhibitors have been synthesized and tested in the hope to find a better clinical drug for cancer therapy. A large number of structurally diverse colchicine binding site inhibitors molecules display their anticancer activity based on their abilities to arrest cell<sup>5</sup>.

Due to the number of cancer cases increases rapidly in the world, it is essential to investigate several successful and affordable cure approaches for the fatal disease, which is also one of the important contributors to the deaths worldwide. Among a variety of ways, the improvement of natural products have been one of the most effective approaches to confirm new points and pipelines<sup>6,7</sup>. Natural products are an considerable source of various bioactive principal compounds for the antitumor drugs, which have excellent significance to the development of the pharmacon<sup>6</sup>.

As a naturally occurring cyclolignan, Podophyllotoxin (PPT, **1**, **Fig.1**) displays cytotoxic activity by inhibition of

microtubule assembly<sup>8,9</sup> through acts at the colchicine binding site on tubulin<sup>10</sup>. Podophyllotoxin has the capabilities of antineoplastic and antiviral<sup>11</sup>, whereas its antimetabolic activity has attracted much attention from investigators<sup>12</sup>. Due to unacceptable toxicity, low bioavailability and gastrointestinal side effects of podophyllotoxin, its clinical application as a drug in cancer chemotherapy has deserted<sup>13</sup>. Consequently, the structural modifications of PPT have been carried out in recent years and have become an interest of anticancer research<sup>14</sup>. Until now, many structural modifications of podophyllotoxin have been synthesized, leading to the development of several clinically beneficial compounds including etoposide (2), teniposide (3) and the water-soluble prodrug etopophos (4) (**Fig. 1**). These podophyllotoxin semisynthetic derivatives used in the treatment of a variety of malignancies, small-cell lung cancer, lymphoma, neuroblastoma, testicular cancer, Ewing's sarcoma and Hodgkin's disease<sup>15, 16</sup>. At the same time, several other derivatives, such as GL-331, NK-611, NPF and TOP-53, are in late stage clinical trials for treating different tumors.

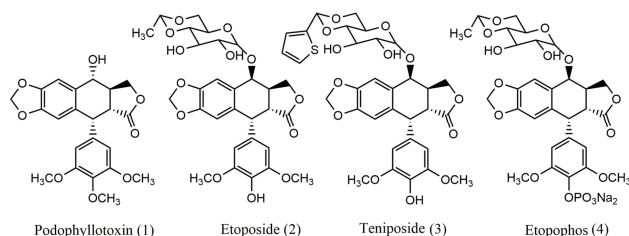


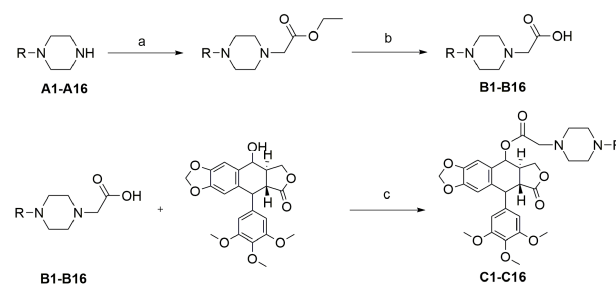
**Fig. 1** Chemical structures of podophyllotoxin derivatives

Piperazine, a N-containing heterocycle with remarkable six membered, is the second most continual ring existing in all FDA approved medications until 2013<sup>17</sup>, which has significant crucial and privileged position in medicinal chemistry<sup>18</sup>. Besides, the existence of this heterocycle can be witnessed in multiple distinguished drugs, which pertains to varying pharmacological action<sup>19</sup>. Piperazine and its derivatives displayed a broad spectrum of biological activities, such as anti-tubercular<sup>20</sup>, antibacterial<sup>21</sup>, antimalarial<sup>22</sup>, especially anti-cancer<sup>23, 24</sup>. Moreover, it can boost the antitumor activity of other anti-cancer drugs.

Above all, we performed a series of podophyllotoxin derivatives through introducing piperazine groups and evaluated their anticancer activities. Therefore, through systematically investigating the chemical structure of the compounds with antitumor activity relationship and exploring its action mechanism, we expect that the present study can further provide theoretical clue for element design of this kind of antitumor drug.

In the preliminary study, we synthesized the intermediate acid, as shown in **Scheme 1**. Then, we use the

carboxylic acids to prepare a series of podophyllotoxin derivatives (**Scheme 1**). These synthetic compounds were presented in **Table 1 (in the Supplementary data)** and their <sup>1</sup>H NMR and ESI-MS results were consistent with the assigned structures, which were reported in the **Supplementary data**. In addition, these compounds were accounted for and characterized for the first time by <sup>1</sup>H NMR, elemental analysis, melting test, and mass spectroscopy, with the results in accordance with the depicted structures.



**Scheme 1** General synthesis of **C1-C16**. Reagents and conditions: (a) ethyl bromoacetate, NaHCO<sub>3</sub>, acetone, reflux, 24 h; (b) NaOH, ethanol, water, 70 °C, 4 h; (c) DCC, DMAP, CH<sub>2</sub>Cl<sub>2</sub>, 20 °C, 8 h.

All the synthesized compounds **C1-C16** were evaluated for anti-proliferative activity against four human cancer cell lines (human breast cancer MCF-7 cells, human cervical carcinoma HeLa cells, human lung adenocarcinoma A549 cells, human hepatoma HepG-2 cells) and one normal cell line human liver L02 cells in vitro by MTT assay. Podophyllotoxin and etoposide were taken as positive drugs. The results were presented in **Table 2 (in the Supplementary data)**. From the data listed, it seemed that almost all the compounds shown the activity of anticancer and it could be found that to compounds **C1-C16**, the substituent groups on the aromatic ring affected the activity remarkably, according to the structure-activity relationship, we clearly found that compounds with substitution on the phenyl ring of the phenylpiperazine group in general exhibited inhibitory activities, electron-withdrawing groups (F, Cl, NO<sub>2</sub>, CF<sub>3</sub>) > electron-donating groups (OMe, Me), and modification of the 2- or 4-position of this phenyl ring led to reduction in potency. Compounds **C2-C5** with chlorine groups on phenyl ring exhibited inhibitory activities in the order of di-substituted > mono-substituted. Moreover, compounds **C14-C16** which have a benzhydryl group exhibited a medium increase in activity comparing to **C1**. Taken together, we selected **C5**, which displayed the most potent MCF-7 inhibitory activity with IC<sub>50</sub> of 2.78 ± 0.15 μM, the best candidate for cancer treatment in this study, for further investigation.

To elucidate whether the cytotoxicity induced by the derivatives was due to cell cycle arrest, we performed flow cytometry analysis for derivatives that exhibited the most potent cytotoxicity. MCF-7 cells were treated with **C5** at 0, 0.3, 0.6 and 0.9  $\mu\text{M}$  as well as podophyllotoxin for 12 h. According to the data annotated in **Fig. 2**, treatment of MCF-7 cells with compound **C5** led to G2/M arrest in a dose-dependent manner. When the concentration of compound **C5** increased to 0.9  $\mu\text{M}$ , 81.03% of cells were arrested in the G2/M phase. We also found that compound **C5** could lead more cells arrested in the G2/M phase than podophyllotoxin (**Fig. 2**). Meanwhile, we designed a time-dependent assay, cells treated with 0.6  $\mu\text{M}$  for different times (0, 4, 8, 12, 16 h) were observed (**Fig. 3**). The analysis performed by flow cytometry showed that the percentage of the cells that arrested in G2/M phase significantly increased with prolongation of the exposed time. Maximum accumulation of 85.57% cells in the G2/M phase was observed after treatment with 0.6  $\mu\text{M}$  of **C5** for 16 h. While, only 62.20% cells arrest in G2/M phase even the concentration of podophyllotoxin increased to 0.6  $\mu\text{M}$  for the same time. These results indicated that the effect of **C5** on cell cycle distribution was better than podophyllotoxin. It revealed that **C5** could interfere with cell proliferation by blocking cell cycle in MCF-7 cells in both dose- and time-dependent manner.

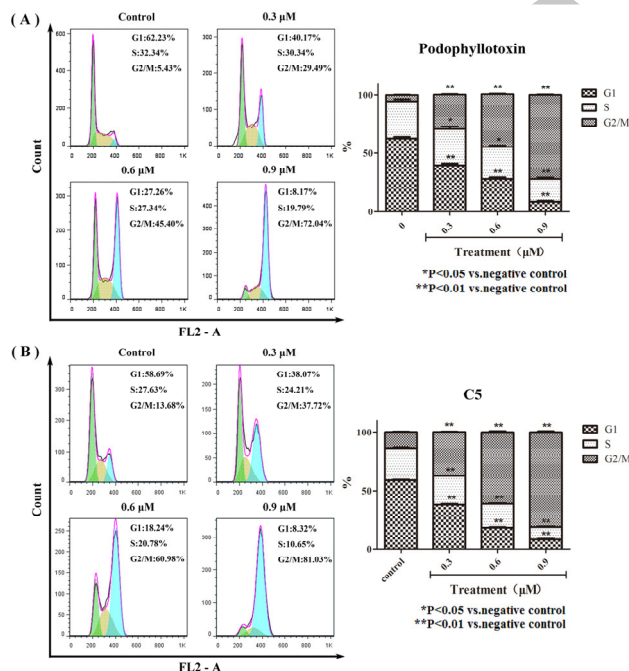


**Fig. 2** Effects of different concentrations of compound **C5** and podophyllotoxin on the cell cycle distribution of MCF-7

cells. **(A)** Cells were treated with 0, 0.3, 0.6, 0.9  $\mu\text{M}$  podophyllotoxin for 12 h. **(B)** Cells were treated with 0, 0.3, 0.6, 0.9  $\mu\text{M}$  **C5** for 12 h. Images are representative of three independent experiments. (G1 phase, green; S phase, yellow and G2/M phase, blue). Data are mean  $\pm$  S.E.M. of three independent experiments. (\* $P < 0.05$ , \*\* $P < 0.01$  compared to control).

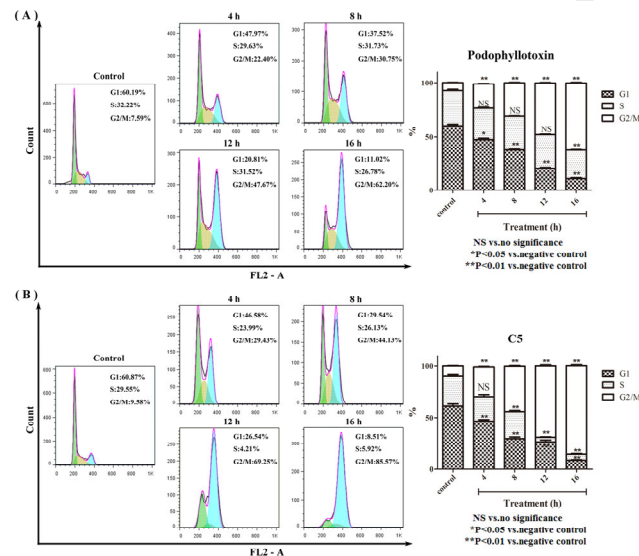


**Fig. 3** Effects of compound **C5** and podophyllotoxin on the cell cycle distribution of MCF-7 cells for different time. **(A)** Cells were treated with 0.6  $\mu\text{M}$  podophyllotoxin for 0, 4, 8, 12, 16 h. **(B)** Cells were treated with 0.6  $\mu\text{M}$  **C5** for 0, 4, 8, 12, 16 h. Images are representative of three independent experiments. (G1 phase, green; S phase, yellow and G2/M phase, blue). Data are mean  $\pm$  S.E.M. of three independent experiments. (\* $P < 0.05$ , \*\* $P < 0.01$  compared to control).

Subsequently, apoptosis was measured by Annexin V/PI double staining by flow cytometry. MCF-7 cells were seeded per well in six-well plates and were treated with **C5** of different concentration (0, 2, 4, 8 and 12  $\mu\text{M}$ ) for 24 h. It is shown that with the increase of the concentration of **C5** in **Fig. 4**. The sensitivity of apoptosis in MCF-7 shows no significant changes, only leads to 37.9% cell apoptosis even at the highest concentration. We predict that it is not an efficient way of **C5** to induce cell death by the effect on cell apoptosis.

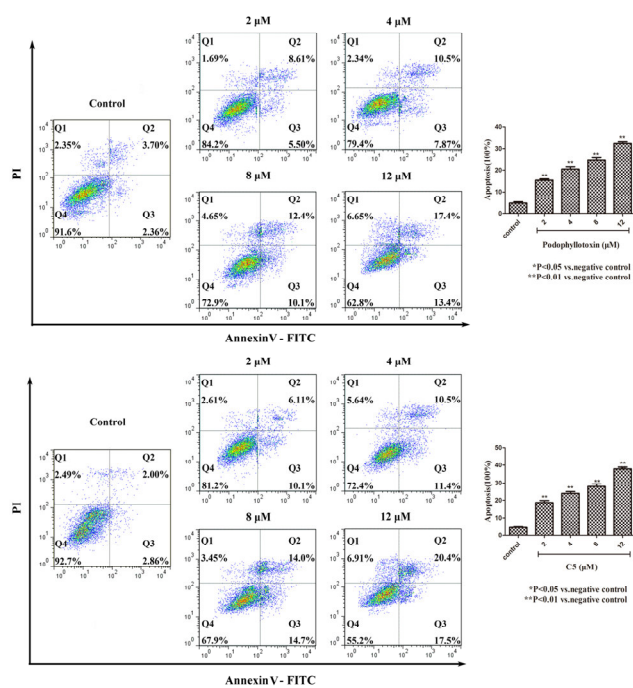


**Fig. 4** Annexin V/PI dual-immuno-fluorescence staining after treatment with podophyllotoxin and different concentrations of for 24 h revealed a moderate increased number of apoptotic and necrotic cells (measured with Annexin V+/PI+ cells). Cells treated with 0, 2, 4, 8, 12  $\mu\text{M}$  podophyllotoxin and **C5** were collected and processed for analysis. The percentage of early apoptotic cells in the lower right quadrant (annexin V-FITC positive/PI negative cells), as well as late apoptotic cells located in the upper right quadrant (annexin V-FITC positive/PI positive cells). Images are representative of three independent experiments. Data are mean  $\pm$  S.E.M. of three independent experiments. (\* $P < 0.05$ , \*\* $P < 0.01$  compared to control)

To examine the safety of these compounds, all of the obtained compounds were evaluated for their toxicity against human liver cells (L02) with the median cytotoxic concentration ( $\text{CC}_{50}$ ) data using the MTT assay. As shown in **Table 2 (in the Supplementary data)**, these compounds were tested at multiple doses and the results demonstrated that most of the analogues possessed low cytotoxicity activities *in vitro* against L02 cells. In particular, the toxicity shown by **C5** molecule against L02 cells is much lower than that of etoposide.

To confirm the effect of **C5** on the cell cycle arrest, western blot analysis was performed to detect the cell cycle-related proteins. As known to us, cyclins, CDKs were as the cell endogenous factor, which involved in cell cycle

regulation. We used this assay to understand the underlying mechanism(s) of cell cycle arrest induced by compound **C5**. The MCF-7 cells treated with compound **C5** at different dose levels (0, 0.5, 1 and 2  $\mu\text{M}$ ), and the final results were shown in **Fig. 5**. As revealed by the intensities of the immune-positive bands, the accumulation levels of CDK1 were markedly increased to the control group, which indicating that the G2/M arrest was induced by **C5**. At the same time, the level of cyclin A, cyclin B1 and cyclin D1 were down regulation which is consistent with the cell cycle arrest phenomenon.

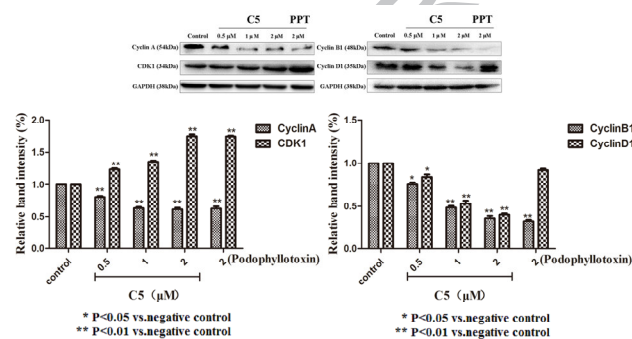


**Fig. 5** Immuno-detection of cell cycle related proteins Cyclin A, Cyclin B1, CDK1 and Cyclin D1 induced cell cycle arrest at G2/M phase in MCF-7 cells. Each band (left to right) represents the treatment using different concentrations (0, 0.5, 1, 2  $\mu\text{M}$ ) of **C5**. And PPT was used as positive control (2  $\mu\text{M}$ ). GAPDH served as a loading control. Images are representative of three independent experiments. Data are mean  $\pm$  S.E.M. of three independent experiments. (\* $P < 0.05$ , \*\* $P < 0.01$ ).

What was more, to further our investigation the phenotypic changes of the cytoskeleton network of tubulin, MCF-7 cells were treated with **C5** and analyzed under confocal microscopy. In brief, MCF-7 cells were treated with **C5** at different concentrations (0, 0.5, 1  $\mu\text{M}$ ), colchicine and paclitaxel at 1  $\mu\text{M}$  for 24 h, respectively and the results as shown in **Fig. 6**. Compared with control group, **C5** could lead to tubulin depolymerization distinctly which is similar to the role of colchicine and with totally different from paclitaxel.

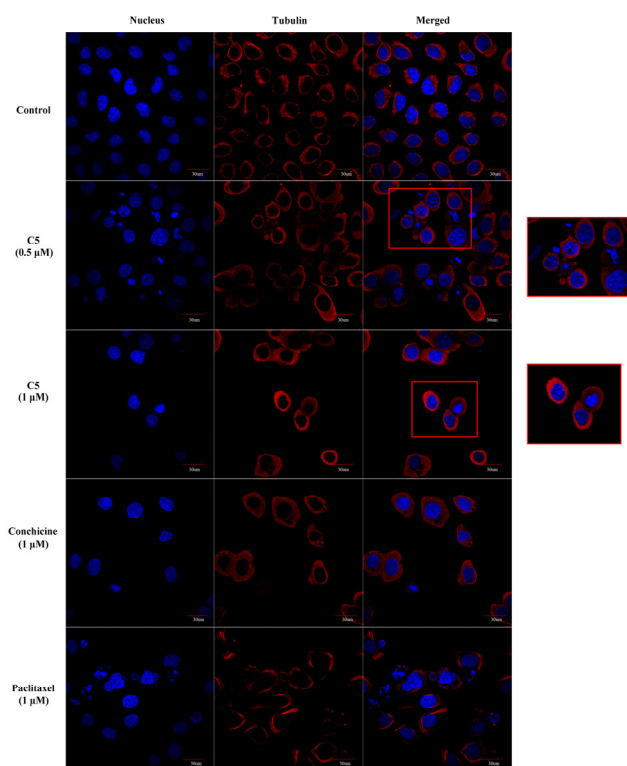


**Fig. 6** Effect of **C5** on the tubulin network of MCF-7 cells using colchicine and paclitaxel as references. Microtubules tagged with rhodamine (red) and nuclei tagged with DAPI (blue) were observed under a confocal microscope.

In this study, the docking simulation was employed iteratively. Podophyllotoxin as the starting point was firstly calculated to predict the binding mode, as detailed in **Fig. 7(A)**. The result revealed that the trimethoxybenzene moiety of podophyllotoxin made a major contribution to the binding affinity, for the strong interactions formed and provided considerable stabilization. As shown in **Fig. 7(B)**, the trimethoxybenzene moiety reached into the deep pocket and formed three Pi-bonds with LEU248, ALA250 and LEU255, respectively. Yet the structure could be optimized to achieve increased binding potency: the outer groove might offer additional interactions when occupied by favorable fragments. Meanwhile, the hydroxyl in methylene offered a considerable modification site. The selection of the suitable fragments can be implemented by means of simulation or empirically. In this work this process was performed automatically by the Scaffold Grow module in DS 3.5, complemented by the docking screening. A set of new molecules were hence constructed and ranked according to the binding energy, with the best hits concomitantly synthesized and initially tested. The lead compound **C5** was then validated. Modification was made to

the lead compound to provide chemical diversity and each of the derivatives were evaluated by bioassays. Also, docking simulation was carried out to compare the variances in the modes and affinities between the starting, the lead and the derivatives, podophyllotoxin. Particularly, **Fig. 7(C)** demonstrated the docking result of **C5** which could combine the tubulin (1SA0) perfectly. It can be concluded that the modification suited our intention as **C5** outperformed podophyllotoxin in binding affinity with 1SA0. The trimethoxybenzene moiety of **C5** remained in the pocket of the tubulin, while its substituent group stretched out and embedded in the groove, which was presented in **Fig. 7(D)**. In addition, the way trimethoxybenzene moiety of **C5** Pi-bonded with the tubulin closely resemble that unsubstituted podophyllotoxin did. The ketone in the dihydrofuran contributed to form one hydrogen bond with ALA250. The phenylpiperazine portion of **C5** is oriented toward the external cavity and formed some interactions, such as Pi-Anion bonds, Alkyl bonds, Pi-Alkyl bonds and Carbon Hydrogen bonds, which contributed to the additional binding affinity of **C5** (-73.3578 kcal/mol). This docking results predicted that the compound **C5** could bind the tubulin (1SA0).

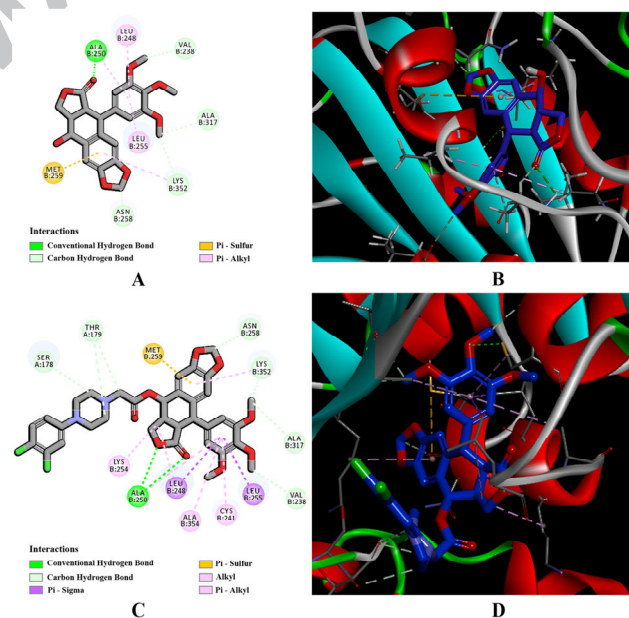


**Fig. 7** Binding modes of podophyllotoxin and **C5** with tubulin (PDB code: 1SA0). (A) 2D image of the interaction between podophyllotoxin and amino acid residues of the active site nearby. (B) 3D image of compound podophyllotoxin inserted in the tubulin binding site. (C) 2D image of the interaction between compound **C5** and amino acid residues of the active site nearby. (D) 3D diagram of compound **C5** inserted in the tubulin binding site.

Briefly, sixteen new podophyllotoxin derivatives containing piperazine ring, were synthesized and evaluated for their activities against multi-cancer cells. Most of the compounds could prevent the cancer cells proliferation and displayed low cytotoxicity towards non-cancer cells. Among them, **C5** showed the most significant anti-cancer activity in MCF-7 cells in MTT assay. In addition, **C5** could apparently block cell cycle at G2 phase in a time- and dose-dependent manner. However, this compound exhibited non-significant effect on the cells apoptosis. Besides, the western blot results indicated that the compound could up-regulate the expression of CDK1 protein and down-regulate the Cyclin A, Cyclin B1 and Cyclin D1 proteins. Particularly, our results demonstrate a prominent effect of **C5** inducing cell cycle arrest at G2/M phase. Also, the expression of cell cycle proteins changes which may validate that microtubules are highly crucial in the process of cell division<sup>25</sup>. When the dynamic equilibrium blocks was disrupted, changes of protein expression occurred. Moreover, based on molecular modeling analysis, we can see that the compounds dock to the colchicine binding site of tubulin and meanwhile, the confocal microscopy assay revealed that the compound **C5**, which was just like the colchicine, can inhibit the tubulin polymerization. As a result, these experiments proved **C5** could be a potential anti-cancer candidate.

### Acknowledgements

The authors are grateful to the Program for Changjiang Scholars and Innovative Research Team in University (IRT\_14R27), the National Natural Science Foundation of China (31470384, 31171161, and 31670298), and the Fundamental Research Funds for the Central Universities (020814380002).

### References and notes

- Jordan, M. A.; Wilson, L. *Nat. Rev. Cancer.* **2004**, *4*, 253.
- Stanton, R. A.; Gernert, K. M.; Nettles, J. H.; Aneja, R. *Med. Res. Rev.* **2011**, *31*, 443.
- Chen, J.; Liu, T.; Wu, R.; Lou, J. S.; Dong, X. W.; He, Q. J.; Yang, B.; Hu, Y. Z. *Eur. J. Med. Chem.* **2011**, *46*, 1343.
- Downing, K. H. *Annu. Rev. Cell Dev. Bi.* **2000**, *16*, 89.
- Lu, Y.; Chen, J. J.; Xiao, M.; Li, W.; Miller, D. D. *Pharm. Res-Dordr.* **2012**, *29*, 2943.
- Newman, D. J.; Cragg, G. M. *J Nat Prod.* **2012**, *75*, 311.
- Butler, M. S. *Nat. Prod. Rep.* **2008**, *25*, 475.
- Sk, U. H.; Dixit, D.; Sen, E. *Eur. J. Med. Chem.* **2013**, *68*, 47.
- Ma, Y. Q.; Fang, S. B.; Li, H. H.; Han, C.; Lu, Y.; Zhao, Y. L.; Liu, Y. Q.; Zhao, C. Y. *Chem. Biol. Drug Des.* **2013**, *82*, 12.
- Bohlin, L.; Rosen, B. *Drug Discov. Today.* **1996**, *1*, 343.
- Imbert, T. F. *Biochimie.* **1998**, *80*, 207.
- Gordaliza, M.; Garcia, P. A.; del Corral, J. M. M.; Castro, M. A.; Gomez-Zurita, M. A. *Toxicol.* **2004**, *44*, 441.

- Shang, H.; Chen, H.; Zhao, D. M.; Tang, X. W.; Liu, Y. F.; Pan, L.; Cheng, M. S. *Arch. Pharm.* **2012**, *345*, 43.
- Xu, H.; Lv, M.; Tian, X. *Curr. Med. Chem.* **2009**, *16*, 327.
- You, Y. J. *Curr. Pharm. Design.* **2005**, *11*, 1695.
- Kamal, A.; Hussaini, S. M. A.; Rahim, A.; Riyaz, S. *Expert Opin Ther Pat.* **2015**, *25*, 1025.
- Taylor, R. D.; MacCoss, M.; Lawson, A. D. G. *J. Med. Chem.* **2014**, *57*, 5845.
- Jida, M.; Soueidan, M.; Willand, N.; Agbossou-Niedereorn, F.; Pelinski, L.; Laconde, G.; Deprez-Poulain, R.; Deprez, B. *Tetrahedron Lett.* **2011**, *52*, 1705.
- Cho, S. D.; Song, S. Y.; Kim, K. H.; Zhao, B. X.; Ahn, C.; Joo, W. H.; Yoon, Y. J.; Falck, J. R.; Shin, D. S. *B. Kor. Chem. Soc.* **2004**, *25*, 415.
- Wang, Y.; Ai, J.; Wang, Y.; Chen, Y.; Wang, L.; Liu, G.; Geng, M.; Zhang, A. *J. Med. Chem.* **2011**, *54*, 2127.
- Meher, C.; Rao, A.; Omar, M. *Asian. J. Pharm. Sci. Res.* **2013**, *3*, 43.
- Ibezim, E.; Duchowicz, P. R.; Ortiz, E. V.; Castro, E. A. *Chemometr. Intell. Lab.* **2012**, *110*, 81.
- Chetan, B.; Bunha, M.; Jagrat, M.; Sinha, B. N.; Saiko, P.; Graser, G.; Szekeres, T.; Raman, G.; Rajendran, P.; Moorthy, D.; Basu, A.; Jayaprakash, V. *Bioorg. Med. Chem. Lett.* **2010**, *20*, 3906.
- Akkoc, M. K.; Yuksel, M. Y.; Durmaz, I.; Atalay, R. C. *Turk. J. Chem.* **2012**, *36*, 515.
- Kozielski, F.; Arnal, I.; Wade, R. H. *Current Biology.* **1998**, *8*, 191.

### Figure and table captions:

**Table 1** Chemical structures of **C1-C16**.

**Table 2** The cytotoxicity of compound **C1-C16** against a panel of human cancer cell lines and one non-cancer cell line

**Fig. 1** Chemical structures of podophyllotoxin derivatives

**Fig. 2** Effects of different concentrations of compound **C5** and podophyllotoxin on the cell cycle distribution of MCF-7 cells. (A) Cells were treated with 0, 0.3, 0.6, 0.9  $\mu$ M podophyllotoxin for 12 h. (B) Cells were treated with 0, 0.3, 0.6, 0.9  $\mu$ M **C5** for 12 h. Images are representative of three independent experiments. (G1 phase, green; S phase, yellow and G2/M phase, blue). Data are mean  $\pm$  S.E.M. of three independent experiments. (\*P < 0.05, \*\*P < 0.01 compared to control).

**Fig. 3** Effects of compound **C5** and podophyllotoxin on the cell cycle distribution of MCF-7 cells for different time. (A) Cells were treated with 0.6  $\mu$ M podophyllotoxin for 0, 4, 8, 12, 16 h. (B) Cells were treated with 0.6  $\mu$ M **C5** for 0, 4, 8, 12, 16 h. Images are representative of three independent experiments. (G1 phase, green; S phase, yellow and G2/M phase, blue). Data

are mean  $\pm$  S.E.M. of three independent experiments. (\*P < 0.05, \*\*P < 0.01 compared to control).

**Fig. 4** Annexin V/PI dual-immuno-fluorescence staining after treatment with podophyllotoxin and different concentrations of for 24 h revealed a moderate increased number of apoptotic and necrotic cells (measured with Annexin V+/PI+ cells). Cells treated with 0, 2, 4, 8, 12  $\mu$ M podophyllotoxin and **C5** were collected and processed for analysis. The percentage of early apoptotic cells in the lower right quadrant (annexin V-FITC positive/PI negative cells), as well as late apoptotic cells located in the upper right quadrant (annexin V-FITC positive/PI positive cells). Images are representative of three independent experiments. Data are mean  $\pm$  S.E.M. of three independent experiments. (\*P < 0.05, \*\*P < 0.01 compared to control)

**Fig. 5** Immuno-detection of cell cycle related proteins Cyclin A, Cyclin B1, CDK1 and Cyclin D1 induced cell cycle arrest at G2/M phase in MCF-7 cells. Each band (left to right) represents the treatment using different concentrations (0, 0.5, 1, 2  $\mu$ M) of **C5**. And PPT was used as

positive control (2  $\mu$ M). GAPDH served as a loading control. Images are representative of three independent experiments. Data are mean  $\pm$  S.E.M. of three independent experiments. (\*P < 0.05, \*\*P < 0.01).

**Fig. 6** Effect of **C5** on the tubulin network of MCF-7 cells using colchicine and paclitaxel as references. Microtubules tagged with rhodamine (red) and nuclei tagged with DAPI (blue) were observed under a confocal microscope.

**Fig. 7** Binding modes of podophyllotoxin and **C5** with tubulin (PDB code: 1SA0). (A) 2D image of the interaction between podophyllotoxin and amino acid residues of the active site nearby. (B) 3D image of compound podophyllotoxin inserted in the tubulin binding site. (C) 2D image of the interaction between compound **C5** and amino acid residues of the active site nearby. (D) 3D diagram of compound **C5** inserted in the tubulin binding site.

**Scheme 1** General synthesis of **C1-C16**. Reagents and conditions: (a) ethyl bromoacetate, NaHCO<sub>3</sub>, acetone, reflux, 24 h; (b) NaOH, ethanol, water, 70 °C, 4 h; (c) DCC, DMAP, CH<sub>2</sub>Cl<sub>2</sub>, 20 °C, 8 h.

## Graphical Abstract

**Design and synthesis of piperazine acetate podophyllotoxin ester derivatives targeting tubulin depolymerization as new anticancer agents**

Wen-Xue Sun, Ya-Jing Ji, Yun Wan, Hong-Wei Han, Hong-Yan Lin, Gui-Hua Lu, Jin-Liang Qi,<sup>a,b</sup> Xiao-Ming Wang<sup>a,b</sup> and Yong-Hua Yang<sup>a,b</sup>

<sup>a</sup>State Key Laboratory of Pharmaceutical Biotechnology, NJU-NJFU Joint Institute of Plant Molecular Biology, Nanjing University, Nanjing, 210023, China

<sup>b</sup>Co-Innovation Center for Sustainable Forestry in Southern China, Nanjing Forestry University, Nanjing, 210037, China

It proves mitotic inhibition activities of C5 in MCF-7 cells and Cyclin A, Cyclin B1, Cyclin D1, CDK1 is involved in the mitosis process induced by C5

